Colloids and Surfaces A: Physicochem. Eng. Aspects 430 (2013) 1–7

Contents lists available at SciVerse ScienceDirect

Colloids and Surfaces A: Physicochemical and Engineering Aspects

journal homepage: www.elsevier.com/locate/colsurfa

Influence of relative humidity on spreading, pattern formation and adhesion of a drying drop of whole blood

W. Bou Zeid, D. Brutin*

Aix Marseille University, IUSTI UMR 7343, 13013 Marseille, France

HIGHLIGHTS

- The contact angle linearly decreases with the relative humidity.
- The wetting diameter decreases with the relative humidity.
- Relative humidity changes strongly the pattern formation.
- The evaporation rate is well predicted using a modified diffusion law.

GRAPHICAL ABSTRACT

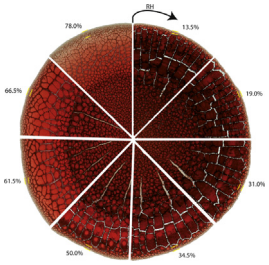

ARTICLE INFO

Article history:
Received 15 January 2013
Received in revised form 1 March 2013
Accepted 4 March 2013
Available online 11 April 2013

Keywords:
Biocolloids
Human blood
Thermocapillary convection
Evaporation

ABSTRACT

The drying of a drop deposited on a solid substrate has been the subject of several investigations including biomedical and forensic fields. These studies also focus on the complex final drop pattern observed at the end of the evaporation process. Our experimental work aims to investigate the effect of relative humidity (RH) on the spreading behavior and on the pattern formation of a dried drop of whole blood at the end of the evaporation process. A range of RH between 13.5% and 78.0% is studied. Drops of blood of same volume are gently deposited on ultraclean microscope glass substrates. A top-view camera allows for the monitoring of the drying regime (deposition, gelation and fracturation). We show that RH influences the contact angle, and the final wetting diameter and consequently, the final deposition pattern at the end of the evaporation process. A good agreement has been observed between our results for whole blood and the experimental work of Chhasatia et al. [Appl. Phys. Lett. 97, 231909 (2010)] performed an aqueous drop of 1.1 μm colloids. Our experimental measurements are in a good agreement with the purely diffusive model where the wetting diameter and the contact angle are function of RH. Our experimental results also show that the transition between the purely convective evaporation phase and the gelation phase occurs always at 65% of the total drying time whatever is the RH levels.

1. Introduction

The patterns observed after the complete desiccation of sessile drop of biological fluid have been the subjects of numerous research studies. In the last few decades, interest to the pattern formation in drying drops of the biological fluids has grown stably (see Table 1), as a result of the increase in the range of few applications: DNA mapping [1], printing and coatings technologies [2,3], manufacturing of new electronic and optical devices [4,5], medical tests [6,9,10], drug screening [11], bio-stabilization [12], and even in forensic investigations.

However, different patterns observed during an evaporating colloidal drop could exhibit a ring-like structure [13], or more complex features such as a network of polygons [14], hexagonal arrays [15] or a uniform deposit [16]. When a small drop of dilute colloidal suspension is dried on a wetted solid substrate, colloidal particles are accumulated at the contact line and a typical drying pattern, the so called "coffee ring", remains. The reason for the formation of such a pattern is the contact line pinning due to the particles suspended

* Corresponding author. Tel.: +33 4 91 10 68 86; fax: +33 4 91 10 69 69.
E-mail addresses: wassim.bouzeid@polytech.univ-mrs.fr (W. Bou Zeid), david.brutin@univ-amu.fr (D. Brutin).

0927-7757/$ – see front matter © 2013 Elsevier B.V. All rights reserved.
http://dx.doi.org/10.1016/j.colsurfa.2013.03.019

Table 1
Literature concerning the evaporation of drops of biological fluids

First author references	Year	Biological fluid	Substrate type	Observations
Yakhno [6]	2008	Human blood serum	Glass	Salt crystallization and protein glass transition
Yakhno [7]	2012	Water solutions	Glass	Thermographic investigation at the drop interface
Tarasevich [8]	2011	Human serum albumin	Glass	dynamics of shape and concentration
Brutin [9]	2011	Human whole blood	Glass	Pattern formation in drying droplet of blood
Zhuang [39]	1982	Human blood serum	Filter paper	Used of dried serum on filter paper
Tarasevich [43]	2007	Biological fluids (Nacl)	–	Modeling with diffusion and convection
Shabalin [44]	2007	Human blood serum	Glass	Pattern differences evidenced for different diseases
Smalyukh [45]	2006	Human DNA solution	Glass	Ringlike deposits formed by drying droplets of DNA
Annarelli [46]	2001	Bovine serum albumin	Glass	Cracks formation in dried droplets of protein serum

in the liquid and the movement of particles and liquid together toward the rim to replenish the liquid that evaporates much faster near the contact line [13]. In fact, the phenomenon of pattern formation in drying drops depends on several parameters such as the physicochemical properties of the solid substrate [17], the spreading behavior [18], the internal flow field (Marangoni convection [14]), the drying conditions (temperature [19], relative humidity of the evaporation environment (RH) [20], air velocity [21]), the presence of surfactant [22,23] and the type of the particles (size [24], chemical composition [25]).

Extensive studies of the evaporation of drops have been undertaken to elucidate the fundammental mechanisms that affect pattern formation notably the effect of the drying conditions. Onoda and Somasundaran [26] showed that the chemical or physical heterogeneities of the substrate influence the final deposition pattern whereas Sobac and Brutin [27] investigated the influence of the substrate surface properties on the evaporation process. Recently, David et al. [28] showed that for same RH, evaporation dynamics and pattern formation of a drop of blood are influenced by substrate wettability. Thus, different contact angles are obtained by using different types of substrates. Also, the final pattern is related to the structure of the particles arrangement caused by change in flow velocity [29] inside the drop and to the internal flow field. Indeed, Marangoni convection inside the drop due to the variation of surface tension along the free surface can affect the deposit formation and the flow fields, as shown by Truskett and Stebe [14]. In 2006, Hu and Larson [16] observed that thermal Marangoni convection induces preferential deposition at the center of the droplet rather than at the periphery for the case of microliter octane drops. It has also been shown that the final deposit pattern can be controlled by the ratio between the substrate and droplet thermal conductivities which controls the direction of Marangoni convection inside an evaporating drop [30].

The competition between the adhesion of the gel onto the substrate and the increasing internal stresses caused by evaporation leads to the formation of a different pattern made up of cracks in order to release the excess of stored elastic energy. Pauchard [31] experimentally studied the influence of the drying rate and the solvent on pattern formation. This pattern is caused by buckle-driven delamination in desiccated colloidal gels. In this study, the author reported that geometrical characterization (cell surface area, radius of curvature and interfacial energy of the buckled region) depends on the drying rate of the gel. Dragneski et al. [20] introduced a new scaling to determine the RH at which cracking occurs. The scaling relates the controlled RH in the humidity chamber to the film thickness. It is suggested that the frequency of cracking and hence the average crack spacing come from balancing the elastic energy released during fracture with the energy required to create the new surface. Also, Pauchard and Allain [32] investigated the surface evolution of drying drops of polymer solution. They showed that the two dominant parameters used to predict surface stability are the initial contact angle and the RH. However, a change in RH would affect the evaporation and the gelation times. Besides, some authors studied the effect of RH in the evaporation time of pinned droplets for various substrate temperatures [33].

An important effect of the atmosphere on the kinetics of evaporation has been also undertaken. Sefiane et al. [34] investigated the effect of the atmosphere and of the ambient gas nature on the evaporation rate of pinned sessile droplets of water. In their study, the evaporation rate was found to increased with reduced atmospheric pressure. Recently, Askounis et al. [35] showed the effect of reducing atmospheric pressure on both the evaporation rate of such a drop (nanoparticles) and on the particle arrangement at the resulting ring-stains.

Only few studies in the literature address the evaporation of sessile drops of biological fluids [6,9,39]. whole blood has seldomly been studied as the target fluid for sessile drop evaporation, though drops of serum have generated several publications. The studies on colloidal sessile drop conducted by Tarasavich et al. [40] focus on the influence of the initial volume fraction of the colloidal particles and the capillary number rather than studying the influence of drying conditions on pattern formation. These parameters are fundamental in studying biological fluids because the fluid phase that evaporates is water. Thus, the understanding of drying conditions on the evaporation dynamics and on pattern formation of a biological fluid in controlled atmospheric conditions is very important in morphological characterization.

Chhastia et al. [41] demonstrated that the particle deposition area and pattern of an aqueous colloidal drops change significantly with the RH. Their analysis showed that the increase in RH result in lower contact angle and more spreading, thereby leads to a larger particle deposition area for the pinned drop. Experiments performed under various RH levels will directly influences the drop evaporation rate, i.e., a drop evaporates faster at lower RH values. With normal atmospheric conditions ($T = 23\,^{\circ}C$, $P = 1013.25$ hPa), Stefans general diffusion theory can be simplified and indicates that the rate of evaporation by diffusion is proportional to the difference between the associated saturation and vapor pressures. Another work regarding drying droplets with colloids of polystyrene spheres of 1 μm in diameter was conducted by Maki and Kumar [42]. They studied the influence of rheological effects on the droplet dynamics and particle distribution. Their method is based on a mathematical model to describe depthwise concentration gradients of the colloids. They conclude that the addition of rheological effects slow down the evaporation dynamics. This is due to the local increase of the viscosity at the contact line where the particles accumulate.

In this article, we will present the influence of the RH on the spreading behavior and on the evolution of cracks pattern. The evaporation rate and the morphological evolutions are clearly influenced by the RH levels.

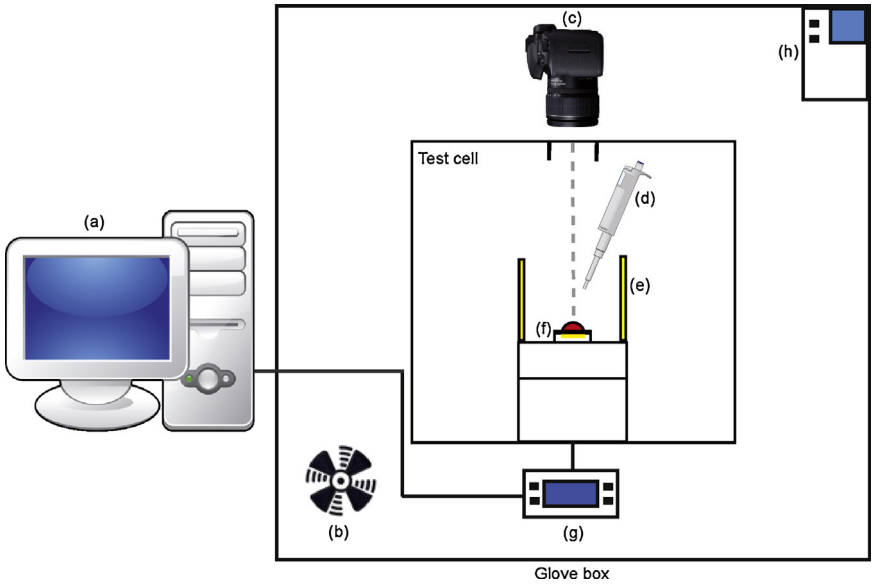

Fig. 1. Equipement used for the evaporation of a sessile drop of blood on glass substrate: a computer (a), a fan to recirculate air inside the box (before the experiment starts) (b), a EOS 7 HD digital camera (c), a digital micropipette (d), two cold light sources (e), a glass substrate (f), a digital balance (g) and a humidity controller (h).

2. Materials and methods

2.1. Experiments

The experiment consists of the spontaneous natural evaporation of a sessile drop of blood under controlled atmospheric conditions and the monitoring of the drying process using a digital highprecision balance with a resolution of 10 μg at 10 Hz (Mettler Toledo XS 105). Simultaneously, visual monitoring was performed using a digital camera (Canon EOS 7D) coupled with a 1–5× macrolens. The digital camera (resolution of 5184 × 3456 pixels on an area of 22.3 × 14.9 mm^3) shoots the top of the drop each 10 s to monitor the evolution of the geometrical parameters related to the drop (i.e, radius, drop height and contact angle). Then, the images are recorded onto a computer disk and analyzed by an image processing system. The optical diagnosis allowed a visualization of the droplet in enough detail for further analysis of specific areas. For the visualization, a cold cathode back light at 5000 K ± 270 K has been used as a unique source of light to avoid reflection on the blood drop interface. The effect of the density of light on the drying process was studied to avoid any biological or chemical disturbance on the phenomenon.

The evaporation is carried out on in a parallelepipedic box measuring 100 × 100 × 150 mm^3 (Fig. 1) which remained covered and the humidity controller is turned off during the experiment to avoid any external flow perturbations and to help reduce noise level.

Blood samples were taken in a nearby medical laboratory and stored in their original 10 μl sterile tubes in a refrigerator at +4 °C in order to be able to perform several experiments at different times within a period of 48 h. Physical properties of blood such as viscosity and surface tension had been determined previously in order to correctly analyze the flow behaviour observed and the pattern formation. The whole blood has been analysed in terms of fluid viscosity using a Physica MCR 501 "Anton Paar" and the surface tension has been determined using the pendant drop method [9]. At the same time, a full haematology and biochemistry analysis of the blood has been performed to obtain the blood characteristics in terms of composition.

RH levels inside the weather station are controlled by supplying either dry or humid air, and a range of investigated RH between 13.5% and 78.0% is obtained during the experiment. The ambient temperature is kept at 23.8 °C for all experiments. Details of the experimental setup are described in Table 2. Drop of blood of volume about 14.2 μl ± 1.0% is injected using a digital micropipette (Eppendorf stream) and gently deposited on an ultra-clean glass substrate, and the drop is allowed to evaporate in an atmosphere composed of air at a temperature T_a of 23.8 °C ± 0.5 °C and a pressure P_a of about 1 bar. The experimental conditions (i.e, temperature T_a, pressure P) are measured using a weather station. We performed several experimental campaigns using the same blood and the same operating conditions. We used first microscope glass substrates clean then ultra-clean. The patterns obtained change slightly depending on the glass cleanness. The results presented below are reproducible and obtained using ultra-clean glass

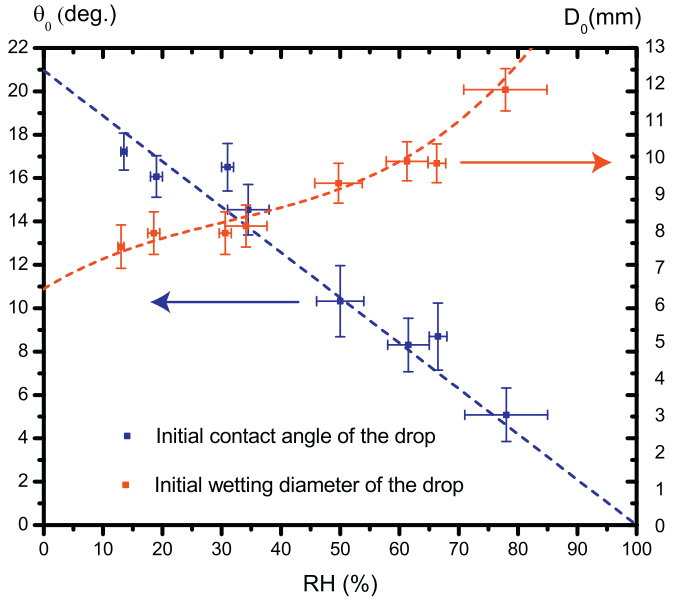

Fig. 2. (Color online) Variation of the initial contact angle θ_0 and the wetting diameter of the drop of blood D_0 as a function of the RH values (room temperature is 23.8 °C ± 0.5 °C and RH varying between 13.5% and 78.0%). The dashed lines are the linear fit for the contact angle (θ_0) and the cubic fit for the wetting diameter (D_0) passing by the measurement points.

Table 2
Experimental details regarding the evaporation of a blood drop of volume $V = 14.2\ \mu l \pm 1.0\%$ on microscope ultra-clean glass substrate with different RH levels.

RH (%)	δRH (%)	m_0 (mg)	δm_0 (%)	D_0 (mm)	δD_0 (%)	θ_0 (degree)	$\delta\theta_0$ (%)	J_0 (μg/s)	δJ_0 (μg/s)
13.5	0.5	13.7	2.2	7.6	0.6	17.2	0.9	6.3	0.6
19.0	1.0	14.7	1.5	8.0	0.6	16.1	1.0	7.1	0.7
31.0	1.0	15.0	1.8	8.0	0.6	16.5	1.1	7.0	0.8
34.5	3.5	14.2	1.9	8.2	0.6	14.5	1.2	5.6	0.3
50.0	4.0	15.0	2.8	9.3	0.5	10.3	1.6	5.1	0.9
61.5	3.5	14.5	1.9	9.9	0.5	8.3	1.2	4.2	0.5
66.5	1.5	14.9	2.6	9.9	0.5	8.7	1.5	4.3	0.5
78.0	7.0	15.1	2.0	11.9	0.6	5.1	1.2	3.5	0.9

substrates only. Volume of drops were kept the same in order to study the influence of RH on the geometrical parameters (contact angle θ_0, wetting diameter D_0). To quantify the increase in deposition area, we calculate the wetting diameter D_0 by using ImageJ.

2.2. Uncertainties

The accuracy of the measured RH values inside the humidity chamber is $\delta = 0.5\%$. As we turned off the humidity controller at the beginning of the experiments to avoid internal convection in the glovebox, values of RH may change at the end of the evaporation process, thereby, each RH value corresponds to the average RH value between two measurements (final and initial). Absolute error of each RH value is estimated by taking the maximum value of the precision of the measuring device and the absolute error of RH value. Experimental values of mass m_0 are calculated from the curve of mass loss while its absolute error from the fluctuated mass at initial time $t = 0$. The absolute error in the measured quantities of wetting diameter D_0 is considered to be 10 pixels for the original image and for the reference image. Finally, values of θ_0 are measured by comparing the experimental volume of blood of drop to the theoretical ones using Eq. (1). Error for this quantities $\delta\theta_0$ is calculated using the maximum and minimum theoretical volume with its uncertainty. Initial evaporative rate J_0 is calculated from a simple derivative of the mass loss.

3. Results

3.1. Influence of relative humidity on spreading and contact angle

Figure 2 shows the theoretically measured contact angle θ_0 as a function of various RH values. Due to the low roughness of the glass substrate and its low surface energy, an hydrophilic behavior of blood on the ultraclean glass substrate is observed with a contact angle θ_0 less than 40°. This contact angle is an apparent angle as opposed to the classical microscopic one which is far below the scale of observation. The drop of blood was deposited onto the substrate and the edge was pinned throughout the drying process. For a small drop with a contact radius of less or about the capillary length, the fluid adopts a spherical cap shape because gravitational forces are negligible. The volume V can be expressed as a function of the contact line radius R_0 and contact angle θ_0.

$$V(R_0, \theta_0) = \frac{\pi R_0^3}{3} \frac{(1-\cos\theta_0)^2(2+\cos\theta_0)}{(\sin^3\theta_0)} \tag{1}$$

Fig. 2 shows also the measured wetting diameter D_0 as a function of RH values. Because the contact line does not recede during the evaporation process, deposition diameter changes slightly at the final time of evaporation t_F resulting in deposition area similar to the initial drop spreading area. The evaporation time t_F is defined as the time for complete evaporation (null mean signal of the drying rate) and for which the mass no longer changes with time during entire evaporation process. This evaporation time t_F is related to the deposition diameter D_0 and can be expressed as below. This total time of evaporation comes from a simplified version of Stephan's law assuming an evaporation mainly driven by convection, diffusion and gelation.

$$t_F = \frac{4RTm_0}{\pi \Delta P D_0 D_{\text{diff}}} \tag{2}$$

where D_{diff} the coefficient of diffusion, T the air temperature, R is the gas constant, m_0 is the initial drop mass, D_0 is the initial wetting diameter, and ΔP is the difference between the saturated pressure and the air pressure.

At 13.5% RH, the final wetting diameter D_0 is 7.6 mm, and this diameter increases with increasing RH. The typical contact angle θ_0 extracted from Fig. 2 are, respectively, 17.2° for 13.5% of RH and 5.1° for 78.0% of RH. One can notice that a linearly increase in the contact angle θ_0 (constant contact-area-mode) leads to a decrease in the wetting diameter D_0 of the drop of blood for higher evaporation rates (lower RH).

We can provide the contact angle variation with RH in Eq. (3) and the wetting radius with RH in Eq. (4).

$$\theta_{\text{RH}} = 21(1 - \text{RH}) \tag{3}$$

Hence, substituting Eq. (3) into Eq. (1), yields the equation R_0 as a function of RH:

$$R_{\text{RH}} = \left(\frac{3V}{\pi} \frac{\sin^3\theta_{\text{RH}}}{(2+\cos\theta_{\text{RH}})(1-\cos\theta_{\text{RH}})^2} \right)^{1/3} \tag{4}$$

3.2. Influence of relative humidity on pattern formation

The influence of RH on the pattern at the end of the drying phase has been investigated by considering same volume of drops of blood evaporating in different RH levels. Final drop images are presented in Fig. 3 which shows morphological and structural evolutions of a drying drop of whole blood for different values of RH. For each RH, bottom-view images are taken at the final evaporation time t_F of the drying phase. In the case of constant area mode and for contact angle less than 90°, Hu and Larson experimentally investigated the evaporation of a sessile droplet by using the finite element method [16]. Thus, they obtained an analytical expression of the rate mass lost from a drop for any contact angle:

$$J_{HL0} = \frac{\mathrm{d}m}{\mathrm{d}t} = \pi R_0 D_{\text{diff}} C_v (1 - \text{RH}) f(\theta) \tag{5}$$

where R_0 is the radius of the drop, D_{diff} the diffusion coefficient (for drop of blood evaporating into surrounding air at 1013.25 hPa and 23.8 °C, this coefficient is $2.19 \times 10^{-5}\ \text{m}^2/\text{s}$), $C_v(1 - \text{RH})$ is the vapor concentration difference between the saturated vapor at the apex and the vapor concentration in the far-field from the drop and $f(\theta) = 0.27\theta^2 + 1.30$ is a function that depends of the contact angle for θ less than 90°. For contact angles below 40°, the function of the contact angle $f(\theta)$ is almost flat. The influence of the contact angle is negligible, and the net evaporation rate from the droplet remains almost constant with time, even though the evaporation flux becomes more strongly singular at the edge of the drop as

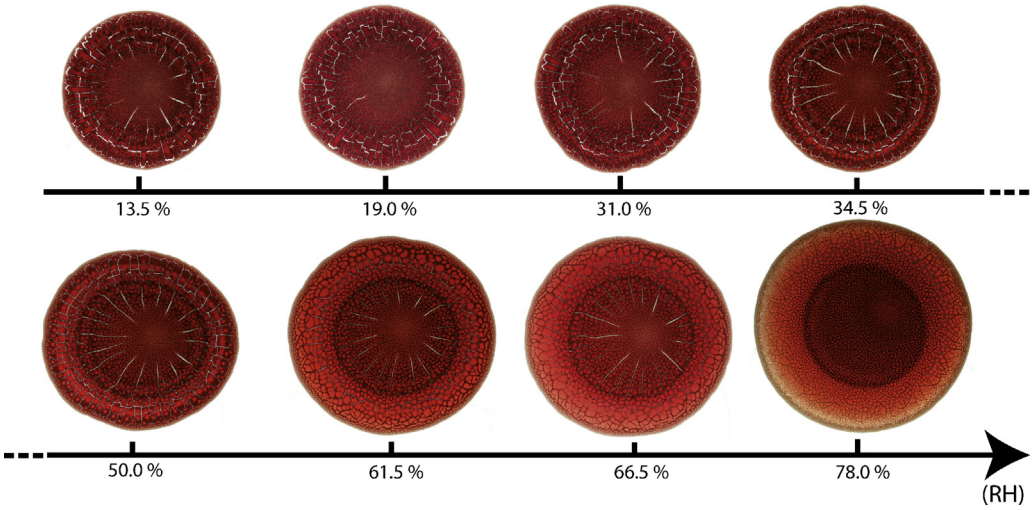

Fig. 3. Top-view images (same scale) of deposit left behind after the complete evaporation of a sessile drop of whole blood. All experiments are performed for same drop volume (V=14.2 μl) and for various range of relative humidity RH (microscope ultraclean glass substrate, room temperature: 23.8 °C, room pressure: 1005 hPa).

the contact angle decreases during evaporation. Thus, the equation above Eq. (5) demonstrates that the evaporation flow rate depends on vapor concentration difference $C_v(1 - \mathrm{RH})$ when evaporating at different values of RH. Using Eq. (3), $f(\theta)$ can be written as:

$$f_{\mathrm{RH}} = (3.59 \times 10^{-2})\mathrm{RH}^2 - (7.18 \times 10^{-2})\mathrm{RH} + 1.33 \quad (6)$$

As the contact angle decreases as a function of the evaporation rate and for the contact angles below 40°, $f(\theta)$ is almost constant and can be approximated to 1.33. Hence, Eq. (5) is expressed as:

$$J_{\mathrm{blood}} = \pi R_{\mathrm{RH}} D_{\mathrm{diff}} C_v (1 - \mathrm{RH}) f_{\mathrm{RH}} \quad (7)$$

In Fig. 3, we clearly observe a structural change and consequently, the morphological evolutions of the final drying pattern. When the evaporation of the drop of blood is completed, the final pattern is characterized by the presence of three distinguished regions (Fig. 3): a central part composed by a sticking deposit and a network of small cracks, a corona composed by wide mobile plaques with white cracks organized radially, a fine periphery completely adhering to the substrate. It can be observed that the width of mobile plaques of the corona and the fine periphery region becomes larger as the RH increases. Moreover, mobile plaques of the corona are more displaced toward the center of the drop leaving a wider deposit made of plaques with dark cracks. Also, Fig. 3 shows that mobile plaques depends on the drying rate. At low drying rates (high RH), complete adhering mobile plaques is observed than at high drying rate (lower RH). Indeed, low adhering areas are highlighted by the circulated red light region which are included in each mobile plaques of the corona area. In the next section, more details will be provided regarding the differences in between crack patterns.

4. Discusion

Upon gentle impact on the ultra-clean glass substrate, the drop of blood spreads to its maximum radius with a contact line velocity proportional to the evaporative rate J_0. However, the contact line velocity decreases and the time interval that the drop spends in the pinned stage of the evaporation increases in the case of drop of blood evaporated at lower evaporative rates (high RH). Also, the contact angle θ_0 decreases for each RH value because of continued contact line pinning and evaporation. Observed higher wetting diameter at lower evaporative rates can be attributed to a lower contact angle during spreading of the drop. These observations are in good agreement with the work of Chhasatia et al.[41], who showed experimentally that RH affects the contact angle and spreading behavior of an aqueous colloidal drop. The physical explanation proposed is based on the contact line velocity during the initial spreading which is affected by the evaporation rate at the contact line. The contact angle equilibrium model does not take into account of the evaporation at the triple line. If we consider a contact line with colloids under evaporation then the force balance is modified and the new equilibrium contact angle is affected by both the colloids and the evaporation rate. The colloids act by helping to pin the contact line such as high evaporation rate. The authors introduced a function that relates the dynamic contact angle to the evaporative rate by using the previous empirical studies in the litterature of the spreading of nonvolatile liquids.

The evolutions of the initial evaporative rates are presented in Fig. 4. The evaporation time has been scaled by the final evaporation time t_F for each RH value. Typically, at 13.5% RH, the evaporation rate is higher than that at 78.0% RH. For all curves presented in Fig. 4, evaporated drops of blood have almost the same dynamics. The curves of the initial evaporative rate evidence a first regime mainly driven by convection with a transition phase that indicates

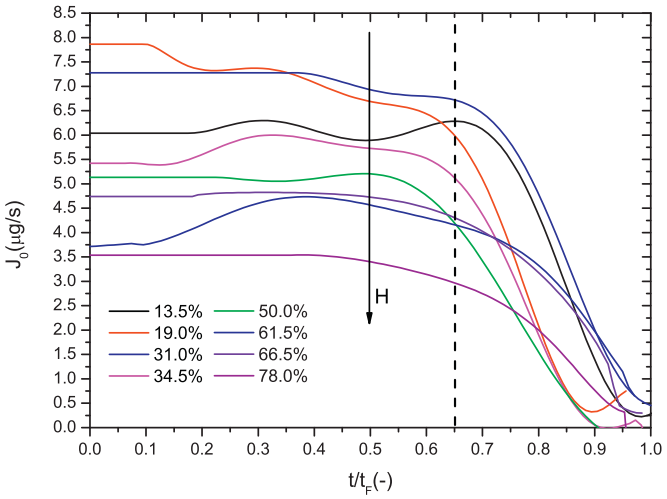

Fig. 4. Evolution of the initial evaporative mass flux J_0 of drops of blood of volume V = 14.2 μl ± 1% for investigated humidities ranging from 13.5% to 78.0% vs the dimensionless time t/t_F.

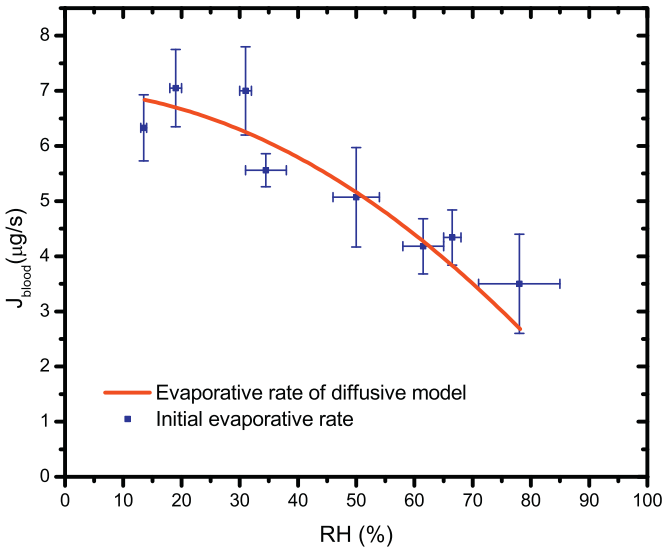

Fig. 5. Variation of the initial evaporative rate as a function of the RH: experimental results (points) and theoretical model (line).

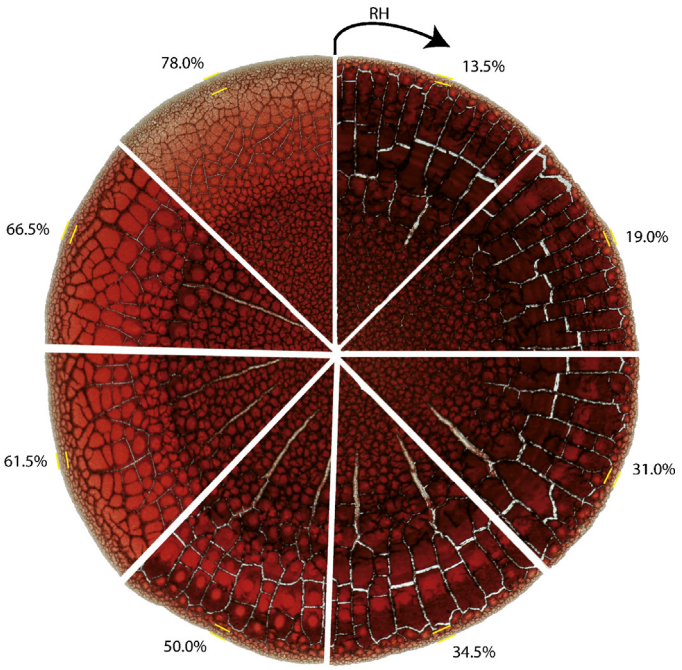

Fig. 6. Final deposition morphology for a various RH values (RH varying between 13.5% and 78.0%). Area between dashes in yellow represents the fine periphery corona.

the complete gelation of the system. Regardless of the RH levels, the transition between these two regimes occurs at about 65% of the total drying time.

It is clear that, when increasing the values of RH, the environment of the studied drops of blood becomes more saturated with vapor concentration. The effect of diffusion of the molecules is lowered and thus the kinetics of evaporation slows down. However, evaporation time increases and important dependance with the RH shows up. Fig. 5 illustrates the effect of the variations of both the contact angle and the wetting diameter on the evaporative rates. It can appears that our experimental results evidence good correlation with the theoretical diffusive model which decreases with RH. This result shows a strong dependance of the initial evaporative rate also due to the RH effect on θ_0 and D_0.

The final drying pattern and crack nucleation vary with the kinetics of the evaporation rate as presented in Fig. 6. Under our experimental conditions, the transfer of water in air is limited by diffusion and is controlled by the RH in the surrounding air. The drying process of a sessile drop of blood is charactarized by an evolution of the solution into a gel saturated with solvent. When the gel is formed, the new porous matrix formed by the aggregation of particles continues to dry by evaporation of the solvent which causes gel to consolidate. As the liquid progressively recedes into the porous medium, it forms at first menisci at the air/solvent interface due to capillary tension between the particles and then causes liquid bridges between the particles. During solvent evaporation curvature of the solvent-air menisci is responsible for a capillary pressure, P_{cap}, in the liquid phase. The maximum capillary pressure in the gel can reach:

$$P_{cap} = \frac{\alpha\gamma_{(s,a)}\cos(\theta)}{r_p} \quad (8)$$

where $\gamma_{(s,a)}$ is the solvent-air surface tension, θ is the liquid/solid contact angle, r_p the pore radius and α is a geometrical constant with a value of 10 approximately [47]. This depression induces shrinkage of the porous matrix that is constrained by the adhesion of the deposit to the glass substrate and the evaporation of solvent. As tensile stresses builds up, the internal stresses become too great and fractures appear so as to release mechanical energy. Assuming that gelation is due to particles accumulation, we attribute these differences in pattern formation to the competition between the drying process and the adhesion of the gel on the substrate. Final dried images presented in Fig. 6 show that the final adhering surface area of mobile plaques is strongly dependent on the RH values. By changing the drying rate, the mechanical properties of the drying gel are modified such as the adhesion energy of the gel to the glass substrate (according to Griffith theory). Indeed, surface area of mobile plaques of drops of blood dried at RH from 13.5% to 50.0% becomes progressively larger with a lower adhering region. This adhering region shrinks until the formation of a circular adhering region which leads to a delamination process. For images of RH above 50%, mobile plaques are smaller with a higher adhering region. This observation is due to the buckling process that is rapidly overcome by the adhesion of the gel to the substrate. In desiccated colloidal gel dried at RH = 70% and RH = 46%, Pauchard [31] experimentally showed that complete adhesion or de-adhesion is function of the cell surface area. Moreover, the large fine periphery of the stick deposit onto the glass substrate (see Fig. 6) is due to the receding of gel front causing the absence of red blood cells (RBCs). This result is due to change in internal flow that transports RBCs from the center to the periphery of the drop of blood.

5. Concluding remarks

The influence of RH on the spreading behavior and pattern formation is studied. Drops of blood of same volume are deposited on an ultraclean glass substrate and evaporated inside a humidity chamber with a controlled range of RH between 13.5% and 78.0%. Our experiments show that the contact angle decreases as a function of the RH which influences the final deposition pattern at the end of the evaporation process. Due to the effect of RH on the contact angle of the drop of blood, initial evaporative rate is dependent of RH values. Observed cracks pattern at the end of the drying process is due to the competition between the drying regime and the gelation inside the drop of blood. Also, the transition between the purely convective evaporation regime and the gelation regime appears always at 65% of the total drying time. Thus, controlling

evaporative rate by evaporating drop of blood in different RH levels impact strongly the wettability properties and the final pattern of drying drop of blood.

References

[1] J. Jing, J. Reed, J. Huang, X. Hu, V. Clarke, J. Edington, D. Housman, T.S. Anantharaman, E.J. Huff, B. Mishra, B. Porter, A. Shenker, E. Wolfson, C. Hiort, R. Kantor, C. Aston, D.C. Schwartz, Automated high resolution optical mapping using arrayed, fluid-fixed DNA molecules, Proc. Natl. Acad. Sci. U.S.A. 95 (1998) 8046–8051.

[2] D. Kim, S. Jeong, B.K. Park, J. Moon, Direct writing of silver conductive patterns: improvement of film morphology and conductance by controlling solvent compositions, Appl. Phys. Lett. 89 (2006) 264101.

[3] J. Park, J. Moon, Control of colloidal particle deposit patterns within picoliter droplets ejected by ink-jet printing, Langmuir 22 (2006) 3506–3513.

[4] T. Kawase, H. Sirringhaus, R.H. Friend, T. Shimoda, Inkjet printed via-hole interconnections and resistors for all-polymer transistor circuits, Adv. Mater. 13 (2001) 1601–1605.

[5] D.J. Norris, E.G. Arlinghaus, L. Meng, R. Heiny, T. Scriven, Opaline photonic crystals: how does self-assembly work? Adv. Mater. 16 (2004) 1393–1399.

[6] T. Yakhno, Salt-induced protein phase transitions in drying drops, J. Colloid Interface Sci. 318 (2008) 225–230.

[7] T.A. Yakhnoa, O.A. Saninaa, M.G. Volovikb, A.G. Sanina, V.G. Yakhnoa, Thermographic investigation of the temperature field dynamics at the liquid-air interface in drops of water, Zhurnal Tekhnicheskoi Fiziki 22–29 (2012) 82.

[8] Yu. Tarasevich Yuri, V. Vodolazskaya Irina, P. Isakova Olga, Desiccating colloidal sessile drop: dynamics of shape and concentration, Colloid Polymer Sci. (2011).

[9] D. Brutin, B. Sobac, B. Loquet, J. Sampol, Pattern formation in drying drops of blood, J. Fluid Mech. 667 (2011) 85–95.

[10] B. Sobac, D. Brutin, Structural and evaporative evolutions in desiccating sessile drops of blood, Phys. Rev. E 84 (2011) 011603.

[11] Takhistov, H.C. Chang, Complex stain morphologies, Ind. Eng. Chem. Res. 41 (25) (2002) 6256–6269.

[12] V. Ragoonanan, A. Aksan, Heterogeneity in desiccated solutions: implications for biostabilization, Biophys. J. 94 (6) (2008) 2212–2227.

[13] R.D. Deegan, O. Bakajin, T.F. Dupont, G. Huber, S.R. Nagel, T.A. Witten, Capillary flow as the cause of ring stains from dried liquid drops, Nature 19 (1997) 827–829.

[14] V.N. Truskett, K.J. Stebe, Influence of surfactants on an evaporating drop: fluorescence images and particle deposition patterns, Langmuir 19 (2003) 8271–8279.

[15] M. Maillard, L. Motte, M.-P. Pileni, Rings and hexagons made of nanocrystals, Adv. Mater. 13 (2001) 200–204.

[16] H. Hu, R.G. Larson, Marangoni effect reversed coffee-ring depositions, J. Phys. Chem. B 110 (2006) 7090–7094.

[17] D.H. Shin, S.H. Lee, J. Jung, J.Y. Yoo, Evaporating characteristics of sessile droplet on hydrophobic and hydrophilic surfaces, Microelectron. Eng. 86 (2009) 1350–1353.

[18] D. Bonn, Wetting and spreading, Rev. Modern Phys. 81 (2009).

[19] G. Gauthier, V. Lazarus, L. Pauchard, Shrinkage star-shaped cracks: explaining the transition from 90 degrees to 120 degrees, Europhys. Lett. 89 (2010) 26002.

[20] K.I. Dragnevski, A.F. Routh, M.W. Murray, A.M. Donald, Cracking of drying latex films: an ESEM experiment, Langmuir 26 (2010) 7747–7751.

[21] L. Goehring, W.J. Clegg, A.F. Routh, Solidification and ordering during directional drying of a colloidal dispersion, Langmuir 26 (2010) 9269–9275.

[22] R.D. Deegan, Pattern formation in drying drops, Phys. Rev. E 61 (2000) 475–485.

[23] T. Still, P.J. Yunker, A.G. Yodh, Surfactant-induced marangoni eddies alter the coffee-rings of evaporating colloidal drops, Langmuir 28 (2012) 4984–4988.

[24] E.R. Dufresne, E.I. Corwin, N.A. Greenblatt, J. Ashmore, D.Y. Wang, A.D. Dinsmore, J.X. Cheng, X.S. Xie, J.W. Hutchinson, D.A. Weitz, Flow and fracture in drying nanoparticle suspensions, Phys. Rev. Lett. 91 (2003) 224501.

[25] W.P. Lee, A.F. Routh, Why do drying films crack? Langmuir 20 (2004) 9885–9888.

[26] G. Onoda, P. Somasundaran, Two- and one-dimensional flocculation of silica spheres on substrates, J. Colloid Interface Sci. 118 (1987) 169–175.

[27] B. Sobac, D. Brutin, Triple line behavior and wettability controlled by nano coated substrates: influence on sessile drop evaporation, Langmuir 27 (2011) 14999–15007.

[28] D. Brutin, B. Sobac, C. Nicloux, Influence of substrate nature on the evaporation of a sessile drop of blood, J. Heat Transfer 134 (2012) 061101.

[29] A.G. Marin, H. Gelderblom, D. Lohse, J.H. Snoeijer, Order-to-disorder transition in ring-shaped colloidal stains, Phys. Rev. Lett. 107 (2011) 08552.

[30] W.D. Ristenpart, P.G. Kim, C. Domingues, J. Wan, H.A. Stone, Influence of substrate conductivity on circulation reversal in evaporating drops, Phys. Rev. Lett. 99 (2007) 234502.

[31] L. Pauchard, Patterns caused by buckle-driven delamination in desiccated colloidal gels, Europhys. Lett. 74 (2006) 188–194.

[32] L. Pauchard, C. Allain, Stable and unstable surface evolution during the drying of a polymer solution drop, Phys. Rev. E 68 (2003) 05280.

[33] F. Girard, M. Antoni, S. Faure, A. Steinchen, Influence of heating temperature and relative humidity in the evaporation of pinned droplets, Colloids Surf. A 323 (2008) 36–49.

[34] K. Sefiane, S.K. Wilson, S. David, G.J. Dunn, B.R. Duffy, On the effect of the atmosphere on the evaporation of sessile droplets of water, Phys. Fluids 21 (2009) 062101.

[35] A. Askounis, K. Sefiane, V. Koutsos, Martin. Shanahan, The effect of evaporation kinetics on nanoparticle structuring within contact line deposits of volatile drops, Colloids Surf. A (2012).

[39] H. Zhuang, A.G. Coulepis, S.A. Locarnini, I.D. Gust, Detection of markers of hepatitis B infection in serum dried on to filter-paper: an application to field studies, Bull. World Health Organ. 60 (1982) 783–787.

[40] Y. Tarasevish, I.V.B. Vodolazskaya, Desiccating colloidal sessile drop: dynmics of shape and concentration, Colloid Polymer Sci. 289 (2011) 1015–1023.

[41] V.H. Chhasatia, A.S. Joshi, Y. Sun, Effect of relative humidity on contact angle and particle deposition morphology of an evaporating colloidal drop, Appl. Phys. Lett. 97 (2010) 231909.

[42] K.L. Maki, S. Kumar, Fast evaporation of spreading droplets of colloidal suspensions, Langmuir 18 (2011) 11347–11363.

[43] Y.Y. Tarasevich, D.M. Pravoslavnova, Segregation in desiccated sessile drops of biological fluids, Eur. Phys. J. E. 22 (2007) 311–314.

[44] V.N. Shabalin, S.N. Shatokhina, Diagnostic markers in the structures of human biological liquids, Singapore Med. J. 48 (2007) 440.

[45] I.I. Smalyukh, O.V. Zribi, J.C. Butler, O.D. Lavrentovich, G.C.L. Wong, Structure and dynamics of liquid crystalline pattern formation in drying droplets of DNA, Phys. Rev. Lett. 96 (2006) 440.

[46] C.C. Annarelli, J. Fornazero, J. Bert, J. Colombani, Crack patterns in drying protein solution drops, Eur. Phys. J. E 5 (2001) 599–603.

[47] C.J. Brinker, G.W. Scherer, Sol–gel science: the physics and chemistry of sol–gel processing, Academic Press, Boston, 1990.